Toxicological effects of zinc oxide nanoparticle exposure: an *in vitro* comparison between dry aerosol air-liquid interface and submerged exposure systems

Karin Lovén, Julia Dobric, Deniz A. Bölükbas, Monica Kåredal, Sinem Tas, Jenny Rissler, Darcy E. Wagner & Christina Isaxon

View supplementary material ↗

Published online: 12 Feb 2021.

Submit your article to this journal ↗

Article views: 635

View related articles ↗

View Crossmark data ↗

Taylor & Francis
Taylor & Francis Group

ARTICLE

OPEN ACCESS | Check for updates

Toxicological effects of zinc oxide nanoparticle exposure: an *in vitro* comparison between dry aerosol air-liquid interface and submerged exposure systems

Karin Lovén[a,b] (ID), Julia Dobric[b], Deniz A. Bölükbas[c,d,e] (ID), Monica Kåredal[a,f] (ID), Sinem Tas[c,d,e] (ID), Jenny Rissler[a,b,g] (ID), Darcy E. Wagner[c,d,e] (ID) and Christina Isaxon[a,b] (ID)

[a]NanoLund, Lund University, Lund, Sweden; [b]Ergonomics and Aerosol Technology, Lund University, Lund, Sweden; [c]Lung Bioengineering and Regeneration, Department of Experimental Medical Sciences, Lund University, Lund, Sweden; [d]Wallenberg Center for Molecular Medicine, Lund University, Lund, Sweden; [e]Stem Cell Centre, Lund University, Lund, Sweden; [f]Occupational and Environmental Medicine, Laboratory Medicine, Lund University, Lund, Sweden; [g]Bioeconomy and Health, RISE Research Institutes of Sweden, Lund, Sweden

ABSTRACT
Engineered nanomaterials (ENMs) are increasingly produced and used today, but health risks due to their occupational airborne exposure are incompletely understood. Traditionally, nanoparticle (NP) toxicity is tested by introducing NPs to cells through suspension in the growth media, but this does not mimic respiratory exposures. Different methods to introduce aerosolized NPs to cells cultured at the air-liquid-interface (ALI) have been developed, but require specialized equipment and are associated with higher cost and time. Therefore, it is important to determine whether aerosolized setups induce different cellular responses to NPs than traditional ones, which could provide new insights into toxicological responses of NP exposure. This study evaluates the response of human alveolar epithelial cells (A549) to zinc oxide (ZnO) NPs after dry aerosol exposure in the Nano Aerosol Chamber for In Vitro Toxicity (NACIVT) system as compared to conventional, suspension-based exposure: cells at ALI or submerged. Similar to other studies using nebulization of ZnO NPs, we found that dry aerosol exposure of ZnO NPs via the NACIVT system induced different cellular responses as compared to conventional methods. ZnO NPs delivered at $1.0\,\mu g/cm^2$ in the NACIVT system, mimicking occupational exposure, induced significant increases in metabolic activity and release of the cytokines IL-8 and MCP-1, but no differences were observed using traditional exposures. While factors associated with the method of exposure, such as differing NP aggregation, may contribute toward the different cellular responses observed, our results further encourage the use of more physiologically realistic exposure systems for evaluating airborne ENM toxicity.

Introduction

A variety of engineered nanomaterials (ENMs) are produced and used today, and occupational airborne exposure to ENMs are of increasing concern for the health of the workers (Srivastava, Gusain, and Sharma 2015). An example is engineered zinc oxide nanoparticles (ZnO NPs). ZnO NPs are used in solar cells as well as in optoelectronic and electronic nanodevices (Ambade et al. 2009; Kumar and Chen 2008). As ZnO NPs reflect ultraviolet light, they are also extensively used in sunscreens

(Lewicka et al. 2011), and their antibacterial and antifungal activity (Sharma et al. 2010) makes them useful in external antibacterial agents. Around 550 tons are estimated to be produced annually worldwide (Piccinno et al. 2012), making them a NP of major interest. The major route of occupational human exposure during manufacturing and the handling processes of NPs, is through inhalation from a dry aerosol (Basinas et al. 2018).

A range of toxicological effects have been seen after exposure to ZnO NPs (Vandebriel and De Jong 2012). Effects observed after *in vivo* exposure

---

through inhalation in rodents include an increase in granulocytes (Warheit, Sayes, and Reed 2009), total protein, monocyte chemotactic protein (MCP-1) and interleukin 1 (IL-1) concentrations (Chen et al. 2015) in the lungs. Effects after *in vitro* exposures in human alveolar epithelial cells (A549) include decreased cell viability in submerged cultures (Thongkam et al. 2017), induced cytotoxicity in both submerged and air-liquid interface (ALI) cultures (Mihai et al. 2015; Raemy et al. 2012), release of IL-8 in ALI cultures (Stoehr et al. 2015), and up-regulation of messenger ribonucleic acid (mRNA) expression for *IL-8*, granulocyte-macrophage colony-stimulating factor (*GM-CSF*) and *IL-6* in ALI cultures (Lenz et al. 2013). These effects are believed to be due to critical levels of zinc ions in the lysosomes (Mihai et al. 2015). When ZnO NPs are taken up by cells via endocytosis, they are degraded in the acidic environment of the lysosome, causing release of zinc ions. This release can in turn cause lysosomal destabilization and result in leakage to the cytoplasm and damage to other organelles (Cho et al. 2011). In addition to inducing cytotoxic effects on cells, ZnO NPs can inhibit the lung surfactant function independently of the dissolution of the particles into zinc ions, causing acute toxic effects (Larsen et al. 2020).

In vitro cell models are frequently used as a first screening method of possibly toxic exposures, to minimize the use of animal models, and to study the underlying mechanisms resulting in toxic effects seen in *in vivo* studies. Traditional *in vitro* toxicity testing is conducted with submerged cell cultures, where the cells are covered with growth medium and the NPs are added to the medium. However, there are some limitations of these types of exposures including changed physicochemical properties of the NPs when suspended in medium, difficult assessment of the NP dose, and particle losses to the lateral walls of the culture dish (Upadhyay and Palmberg 2018). Additionally, for respiratory exposure models, submerged cells do not resemble the physiological conditions in the lungs and the cells cannot be exposed to airborne NPs. Improved toxicity testing models for respiratory exposures have therefore been developed so that a more realistic exposure of cells at the ALI can be accomplished, mimicking the conditions seen in the lung *in vivo*.

A number of different ALI exposure systems have been introduced recently (Secondo, Liu, and Lewinski 2017; Upadhyay and Palmberg 2018): MINUCELL, VITROCELL, CULTEX, XposeALI, ALICE, NACIVT etc. Most of them (MINUCELL, VITROCELL, XposeALI) deposit particles by diffusion and/or gravitational settling (Lenz et al. 2013; Lucci et al. 2018; Ji et al. 2017), while ALICE uses a cloud settling technique (Lenz et al. 2009). To increase the deposition efficiency of the NPs, a few systems (CULTEX, NACIVT) use electrostatic deposition (Aufderheide et al. 2011; Jeannet et al. 2015). One of these is the Nano Aerosol Chamber for *In Vitro* Toxicity (NACIVT) system. The NACIVT system combines a controlled incubation environment (adjustable relative humidity (RH) and temperature) with a high-efficiency electrostatic deposition. The particles are charged by a unipolar (positive) diffusion charger and the deposition onto the cells is aided by a unipolar electric field. The NACIVT system has previously been used to study toxicological responses after exposure to silver NP (Jeannet et al. 2016; Svensson et al. 2016; Geiser et al. 2017), carbon NP (Jeannet et al. 2016; Geiser et al. 2017), palladium NP, copper NP (Svensson et al. 2016) and e-cigarette smoke (Delaval et al. 2019).

To ensure that the ALI exposure systems can be used for NP exposures, each system needs to be evaluated with different categories of NPs, and comparative studies between traditionally submerged and ALI exposure systems need to be performed. Multiple ALI systems have already been used in such comparative studies, for example MINUCELL (Lenz et al. 2013), VITROCELL (Xie et al. 2012; Panas et al. 2014; Mihai et al. 2015; Loret et al. 2016; Hilton et al. 2019; Medina-Reyes et al. 2020; Mills-Goodlet et al. 2020), XposeALI (Cappellini et al. 2020), and ALICE (Lenz et al. 2009; Stoehr et al. 2015), and most of them have reported more pronounced effects with the ALI exposure systems than with the submerged at similar dose levels. However, a comparison between the NACIVT system and traditional submerged exposure systems has not previously been performed.

The aim of this study was to compare the toxicological responses to ZnO NP exposure in the NACIVT system with two different submerged exposure systems for three different doses on human alveolar epithelial cells. The toxicological

responses in the NACIVT system were also investigated at three different incubation times including 1, 3 and 24 h.

Materials and methods

Nanoparticles

ZnO NPs were purchased from Sigma Aldrich (catalog no. 721077) in a liquid suspension (20 wt% in H_2O). According to the manufacturer, the primary particle diameters were smaller than 100 nm, with a mean size of maximum 40 nm. These particles have previously been used and characterized in several studies, for example by Wang et al. (2013) and Jiang, Aiken, and Hsu-Kim (2015). Wang et al. reported an average particle size of 67 nm in the ZnO NP suspension (by dynamic light scattering (DLS) analysis), and Jiang et al. reported average primary particle diameters of about 20-30 nm and a specific surface area (SSA) of 38 m^2/g of the ZnO NPs. In the current study, the average primary particle size was determined to be 35 nm via Scanning Electron Microscopy (SEM) (Figure S1, supplemental material) and 34 nm via Dynamic Light Scattering (DLS) in cell growth media (Figure S2, and Table S1) and the SSA was estimated to 31 m^2/g (particle analysis methodology described in the section *Determination of deposited dose* and *Particle characterization*). These same particles have been used for both aerosol and submerged cell exposures.

Cell culture

The immortalized human alveolar epithelial cell line A549 was obtained from ATCC, USA. The cells were cultured in T75 flasks in growth medium comprised of Dulbecco's modified Eagle's medium (DMEM) with Ham's nutrient mixture F-12 (Gibco; Thermo Fisher Scientific, USA) supplemented with 10% (vol/vol) fetal bovine serum (FBS) (Sigma, Sweden) and 1% (vol/vol) penicillin/streptomycin (100 units/ml and 100 µg/ml respectively; Gibco; Thermo Fisher Scientific) at 37 °C with 5% CO_2.

Two days prior to NP exposure, 10,000 cells (3×10^4 cells/cm^2) were seeded in 24-well plates on 6.5 mm Transwell inserts (polyester membrane, surface area: 0.33 cm^2, pore size: 0.4 µm, Corning, VWR, Sweden). In short, 100 µl of the cell suspension was dispensed on the insert membrane and incubated

(37 °C, 5% CO_2) for 30 min to allow cell attachment before 1 ml growth medium was added to the well below the insert membrane (basal side of the cells), as seen in the first column in Table 1.

Aerosol exposures in the NACIVT system

Particle preparation and aerosol generation

The suspension of ZnO NPs was diluted in 150 ml water (resistivity 1.25 MΩcm, produced with reversed osmosis and capacitive deionization, VWR, Sweden) to a concentration of 150 µg/ml (low and medium dose) or 600 µg/ml (high dose), as shown in Table 2, and bath sonicated for 5 min (Elmasonic S30H, Elma Schmidbauer GmbH, Germany). The flask with the ZnO NP suspension was connected to an atomizer (from a Condensation Aerosol Generator SLG270, Topas GmbH, Germany), through which filtered compressed air (low dose 1 bar, medium and high dose 5 bar) was run to generate the aerosol (Table 2). The aerosol passed through a dryer and continued to a 5 L mixing volume before reaching the NACIVT system, in which the particles passed through a humidifier (RH 85%, 37 °C) before they were deposited onto the cells by electrostatic deposition (Jeannet et al. 2015).

Cell preparation and exposure

One day after seeding, the growth medium on top (apical side) of the cells was removed by flipping the inserts upside down and pouring out the growth medium, bringing the cells to the ALI (see second column in Table 1). Two days after seeding (24 h at ALI), 24 inserts were moved from the 24-well plate to the NACIVT chamber and provided with 400 µl basal growth medium before they were simultaneously exposed to one of the doses of aerosolized ZnO NPs for 1 h (see third column in Table 1). Prior to the particle exposures, 24 separate inserts were placed in the NACIVT system for 1 h with filtered air (unexposed controls). Three technical replicates were performed for each dose. After 1 h in the NACIVT system, the cells were moved back to the 24-well plate and incubated for 1 h, 3 h or 24 h (see fourth column in Table 1). At these time points (for both unexposed and exposed cells), cell viability (via WST-1 assay described below) was evaluated for cells on 7-8 inserts. Basal medium was also collected at all time points from 6 of the

Table 1. Description of experiments in the three exposure systems NACIVT, SUB(iso) and SUB(growth).

Exposure system	Seeding	Flipping to ALI (24 h after seeding)	Exposure (48 h after seeding)	Analysis			
				1 h	3 h	24 h	
NACIVT	100 µl cell suspension on top of the membrane 1 ml basal growth medium	Apical growth medium removed	1 h exposure to ZnO NP aerosol	WST-1 LDH Cytokines: IL-6, IL-8, TNF-α, MCP-1	WST-1 LDH Cytokines: IL-6, IL-8, TNF-α, MCP-1	WST-1 LDH Cytokines: IL-6, IL-8, TNF-α, MCP-1	
SUB(iso)	100 µl cell suspension on top of the membrane 1 ml basal growth medium	Apical growth medium removed	24 h exposure in isotonic solution	No analysis	No analysis	WST-1 LDH Cytokines: IL-6, IL-8, TNF-α, MCP-1	
SUB(growth)	100 µl cell suspension on top of the membrane 1 ml basal growth medium	No change	24 h exposure in growth medium	No analysis	No analysis	WST-1 LDH Cytokines: IL-6, IL-8, TNF-α, MCP-1	

Schematic images show the cells (dark red) grown in growth medium (light red) on 24-well inserts (surface area: 0.33 cm²). The inserts were flipped 24 h after seeding in two of the exposure systems (NACIVT and SUB(iso)), bringing the cells to the air–liquid interface (ALI). 48 h after seeding, the cells were exposed to zinc oxide nanoparticles (ZnO NPs, yellow) as an aerosol or suspended in isotonic NaCl solution (blue) or growth medium. Metabolic activity was evaluated with the WST-1 assay and cytotoxicity was evaluated with the LDH-assay. Release of the cytokines interleukins IL-6 and IL-8, the tumor necrosis factor, TNF-α, and the monocyte chemotactic protein, MCP-1 were analyzed with Multiplexed Luminex.

Table 2. Exposure parameters in the three exposure systems NACIVT, SUB(iso) and SUB(growth).

Exposure system	Low dose	Medium dose	High dose
NACIVT			
ZnO NP suspension concentration (µg/ml)	150	150	600
Compressed air pressure (bar)	1	5	5
Deposited mass dose (µg/cm^2)	0.2	1.0	3.0
Deposited surface area dose (cm^2/cm^2)	0.06	0.31	0.92
SUB(iso)			
ZnO NP suspension concentration (µg/ml)	10.0	17.6	70.0
Added suspension volume (µl)	20	20	20
Deposited mass dose (µg/cm^2)	0.6	1.1	4.2
Deposited surface area dose (cm^2/cm^2)	0.18	0.34	1.29
SUB(growth)			
ZnO NP suspension concentration (µg/ml)	3.3	5.7	29.8
Added suspension volume (µl)	50	50	50
Deposited mass dose (µg/cm^2)	0.5	0.9	4.5
Deposited surface area dose (cm^2/cm^2)	0.15	0.28	1.38

corresponding wells and 50 µl was directly placed in a transparent 96-well plate and stored at 4 °C until cytotoxicity analysis (LDH assay described below), performed 24 h after exposure. The rest of the basal medium was stored at −80 °C until analysis of the released cytokines. As a positive control for viability and cytotoxicity, one of the unexposed control inserts, at each analysis time point, were treated with 20 µl Lysis solution (Cytotoxicity Detection Kit[PLUS], Roche Diagnostics GmbH, Mannheim, Germany), containing TritonX-100, 1 h before analysis.

Particle characterization

To characterize the ZnO NPs after aerosolization, the particle number concentration and size distribution was continuously measured in parallel to the exposure in the NACIVT, sampled from the mixing volume with a Scanning Mobility Particle Sizer (SMPS: DMA model 3071, TSI Inc., USA and CPC model 3775, TSI Inc., USA) and an Aerodynamic Particle Sizer (APS: model 3321, TSI Inc., USA). The SMPS measured particles in the range 10 to 400 nm with a time resolution of 120 seconds and the APS measured particles in the range 500 to 20,000 nm with a time resolution of 5 seconds.

Additionally, to study the morphology and the primary particle size of the aerosolized ZnO NPs, silicon (Si) wafers were placed in unused inserts in the NACIVT chamber and the system was run in the same way as during the medium and high dose cell exposure for 1 h to deposit the ZnO NPs onto the wafers. The wafers were analyzed by Scanning

Electron Microscopy (SEM) using a Hitachi SU8010 Cold Field Emission SEM (Hitachi, Japan) with an acceleration voltage of 5 kV. Analysis was performed for two wafers per dose, from wells located at different places on the well plate (i.e. not next to each other).

Determination of deposited dose

Three different doses, 0.2 (low), 1.0 (medium) and 3.0 µg/cm^2 (high), were used for the ZnO NP aerosol exposures, comparable to other studies (Lenz et al. 2009; Lenz et al. 2013; Mihai et al. 2015). By changing the ZnO NP mass concentration in the suspension and the pressure of the compressed air into the atomizer, the three different aerosol concentrations were obtained (Table 2). The deposited mass dose for each particle size was calculated using the following equation, adapted from Jeannet et al. (2015):

$$D = \frac{C_M \cdot Q \cdot t \cdot DE}{A}, \tag{1}$$

where D is the deposited mass dose onto the cells (µg/cm^2), C_M is the aerosol mass concentration (mg/m^3), Q is the air flow to each well (0.025 l/min), t is the exposure time (60 min), DE is the deposition efficiency and A is the total cell area on the insert (0.33 cm^2). C_M was calculated from the SMPS number concentration and size distribution assuming spherical particles and a ZnO bulk density of 5.61 g/cm^3. DE was extrapolated from experimentally determined and calculated values in the NACIVT system (Jeannet et al. 2015) for each particle size in
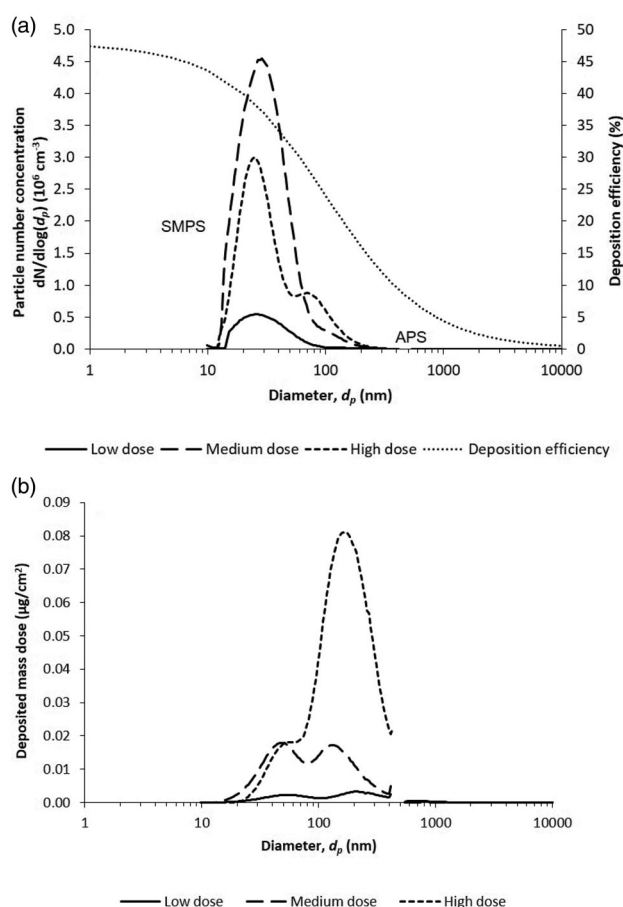
Figure 1. (a) Particle number size distributions of the aerosolized ZnO NPs, measured with the SMPS and the APS (left axis), and the extrapolated deposition efficiency in the NACIVT system from Jeannet et al. (2015) (right axis), and (b) calculated corresponding deposited mass dose size distributions.

the aerosol, fitted by a reciprocal function, see the deposition efficiency curve in Figure 1.

The deposited surface area dose was calculated from the mass dose using a SSA of 31 m^2/g for the ZnO NPs. The SSA was estimated using the ZnO bulk density and an estimated average primary particle size of 35 nm. The average primary particle size was determined from SEM image analysis, described below, of the raw material (liquid suspension) using ImageJ to calculate an average size (details in Figure S1, supplemental material). The deposited surface area doses were determined to 0.06 (low), 0.31 (medium) and 0.92 cm^2/cm^2 (high), as shown in Table 2.

Exposures under submerged conditions

Particle preparation and cell exposure
Two different submerged exposure systems were used, one with 0.9% NaCl isotonic solution

(SUB(iso)) and one with growth medium (SUB(growth)), as seen in Table 1. Preparation of the ZnO NP suspensions was performed a few hours before the exposures. The ZnO NP suspensions were prepared in isotonic solution and growth medium (2550 µg ZnO NP/ml) and bath sonicated for 5 min (Elmasonic S30H, Elma Schmidbauer GmbH, Germany). These ZnO NP suspensions were further diluted to three concentrations (forming three different doses) of ZnO NPs in isotonic solution and in growth medium, as shown in Table 2.

One day after seeding, the apical growth medium for the SUB(iso) exposure was removed by flipping the inserts upside down and pouring out the growth medium, bringing the cells to the ALI (see second column in Table 1). Two days after seeding (24 h at ALI for SUB(iso)), the three different concentrations of ZnO NP suspensions were added to two inserts each. For SUB(iso) exposures, 20 µl of the isotonic ZnO NP suspension was added to the apical side of the cells. For SUB(growth) exposures, the apical growth medium was first removed by flipping the inserts and 50 µl of the growth medium ZnO NP suspensions was then added to the apical side of the cells (see third column in Table 1, and Table 2). Equivalent volumes of particle-free solutions were added to three unexposed control inserts. The low volume of 20 µl in the SUB(iso) exposures was motivated by the intention of resembling ALI as closely as possible (i.e. minimal liquid volume at the apical side of the cells). As a positive control for viability and cytotoxicity, 20 or 50 µl TritonX-100 (1% in growth medium) was added to one of the unexposed control inserts 15 min before analysis. Three technical replicates were performed for both submerged exposure systems. After addition of the ZnO NPs, cells were incubated for 24 h after which cell viability was evaluated and basal medium was collected, of which 50 µl was directly placed in a transparent 96-well plate for cytotoxicity analysis. The rest of the basal medium was stored at −80 °C until analysis of released cytokines (see fourth column in Table 1).

Particle characterization
To characterize the ZnO NPs in suspension, DLS measurements were performed by using a DynaPro Plate Reader II (Wyatt Technology, USA). The measurements were performed in a 96-well plate at

37 °C and ZnO NP concentrations of 1.75 ng/ml to 30 μg/ml in serum-containing growth medium, as described above, and 0.9% NaCl isotonic solution at discrete concentrations used in the current study. Measurements at 1.75 ng/ml in serum-containing growth medium were performed to estimate the size of potential single ZnO NPs. Measurements were made 10 times for each concentration and solvent. All individual measurement outliers were removed via inspection of the Intensity Autocorrelation curves and % Intensity versus hydrodynamic radius were generated with the DYNAMIC 7 Software (Wyatt Technology, USA). Maximum intensity peaks of the histograms were extracted using the DYNAMIC 7 Software.

Additionally, SEM analysis was used to study the morphology and the primary particle size of the ZnO NPs in suspension and in the submerged cell culture systems 24 h after exposure. For morphology visualization, the cells on the membrane inserts were fixed using 2.5% glutaraldehyde solution (Sigma Aldrich, EM grade) with subsequent PBS and water rinsing. The samples then underwent ethanol series dehydration before chemical drying with HDMS (TedPella). Samples were subsequently sputter coated with 5 nm Pt/Pd (80/20) in a Quorum Q150T ES turbo pumped sputter coater and examined with the secondary electron detector at 5 kV and 10 kV in a Jeol JSM-7800F FEG-SEM. To estimate primary particle size via SEM, ZnO NPs from the original stock solution were diluted 1:1000 in water. Individual drops were placed on a SEM stub, allowed to dry, and then imaged using SEM. A grid was overlaid on the SEM image (Figure S1) and the size of the particle closest to the center of each of the 25 squares was measured using ImageJ. The resulting average primary particle size was 35 nm. Of the 25 squares, three had no visible (measurable) particle and the average value is based on 22 measurements.

Determination of deposited dose

The resulting deposited mass doses for SUB(iso) were determined to be 0.6 (low), 1.1 (medium) and 4.2 μg/cm^2 (high). For SUB(growth) the corresponding doses were 0.5 (low), 0.9 (medium) and 4.5 μg/cm^2 (high), as shown in Table 2. The mass doses were calculated from the ZnO NP suspension concentrations multiplied with the added suspension volume, assuming that all particles in the suspension sediment and reach the cell surface as shown by others for ZnO NPs (Lenz et al. 2013; Stoehr et al. 2015). This assumption is based on the larger size determination of the aggregates in the suspension, and the conditions in the current study, with gravitational settling being more dominant than diffusional displacement (further argued in the Discussion section).

The deposited surface area doses in the submerged systems were calculated from the mass doses applying the SSA of the primary particles, determined as described under the section for the aerosol exposures. The surface area doses were for SUB(iso) determined to be 0.18 (low), 0.34 (medium) and 1.29 cm^2/cm^2 (high). For SUB(growth) the corresponding doses were 0.15 (low), 0.28 (medium) and 1.38 cm^2/cm^2 (high), as shown in Table 2.

Viability assay (WST-1)

To evaluate cell viability, as indicated by the level of metabolic activity, the WST-1 assay (Roche Diagnostics GmbH, Germany) was used. The WST-1 cell proliferation reagent was mixed with growth medium (1:10) and after removal of the apical liquids and collection of the basal medium, 110 μl of this solution was added on the apical side of the cells. After 30 min incubation (37 °C and 5% CO$_2$), 100 μl of the solution from each well was moved to a transparent 96-well plate and the absorbance was measured at 450 nm (Multiskan GO Microplate Spectrophotometer, Thermo Scientific, USA, for aerosol exposures, and PHERAstar FS, BMG Labtech, Germany, for submerged exposures).

Cytotoxicity assay (LDH)

Basal medium was analyzed with the Cytotoxicity Detection Kit^{PLUS} (LDH assay; Roche Diagnostics GmbH, Germany) to evaluate cytotoxicity. The assay was performed according to the manufacturer's protocol by mixing the catalyst with the dye (1:45) through vortexing. 50 μl of this solution was then added to each sample of 50 μl basal medium on the transparent 96-well plate. After 30 min incubation in the dark (at room temperature), the absorbance was measured at 490 nm (Multiskan GO Microplate Spectrophotometer, Thermo Scientific,

USA, for aerosol exposures and PHERAstar FS, BMG Labtech, Germany, for submerged exposures).

Cytokine analysis (IL-6, IL-8, TNF-α, MCP-1)

Analysis of the interleukins IL-6 and IL-8, the tumor necrosis factor, TNF-α, and the monocyte chemotactic protein, MCP-1 levels in basal medium was performed with Multiplexed Luminex technology on a Bio-Plex 200 Luminex instrument (Bio-Rad, USA). For each experiment with aerosol exposed and unexposed cells, collected basal medium samples from three wells at each time point were pooled and used for the analysis. For the submerged exposures, the two basal medium samples for each dose from the unexposed and exposed cells were pooled. Components for the assay (plate, standard, antibodies and magnetic beads) were purchased from Bio-Rad and the assay was performed according to the instructions from the manufacturer. Standards, diluted in growth medium, and basal medium samples, undiluted, were analyzed in duplicates on the Luminex plate.

Statistical analysis

All toxicological data are expressed as mean ± standard deviation (SD). The toxicological responses regarding metabolic activity and cytokine analysis were expressed as percent of unexposed controls. The response regarding cytotoxicity was expressed as percent of positive controls (TritonX-100, theoretical maximum LDH release). Significant differences between exposed and unexposed cells were evaluated by a t-test with the hypothetical mean as the unexposed normalized value. Further statistical analysis was performed by one-way analysis of variance (ANOVA). The data was grouped by dose for comparison between exposure systems and grouped by dose and analysis time point for evaluation of the NACIVT system. All statistical analyses were performed using GraphPad Prism 8 and were based on three technical replicates per dose.

Results

Aerosolized particle number size distribution and deposited mass dose in the NACIVT system

In order to determine the doses, the particle number size distributions of the aerosolized ZnO NPs used in the NACIVT exposures were measured with the SMPS and the APS (Figure 1(a)). The count median diameter (CMD) for the ZnO NP aerosol was 29, 29 and 43 nm for the low, medium and high dose, respectively. The calculated corresponding deposited mass dose size distributions are shown in Figure 1(b). The mass dose estimates are based on the measured number size distributions, converted to mass size distributions, and by applying a parameterization of the deposition efficiency, seen in Figure 1(a).

Particle deposition was evenly distributed over the whole wafer surface, as assessed via SEM and both single particles and larger aggregates could be observed (Figure 2(a–d)). In accordance with the SMPS data, the high dose contained more and larger particle aggregates (Figure 2(b,d)) in comparison to the medium dose, which contained more single primary particles and smaller aggregates (Figure 2(a,c)). The estimated primary particle size agrees with the manufacture's specifications, with a primary particle size below 100 nm (Figure 2(c,d)). The aggregate size was estimated to vary between 100-400 nm. Similar size estimates can also be observed in Figure 1(b).

Particle size characterization in submerged conditions

Next, DLS was used to measure ZnO NP sizes in the submerged conditions. Particle size distributions at concentrations below 6.0 μg/ml in growth medium were obtained, while it was not possible to extract reliably quantitative information for particle sizes above this concentration, in either growth medium or isotonic solution (Figure S2 and data not shown). At ultra low concentrations in growth medium (i.e. 1.75 ng/ml), a ZnO NP radius around 34 nm was observed, in agreement with the measurements made using SMPS and SEM (Figure 1 and Figure S1). Larger particle sizes, indicating the formation of aggregates, were observed with a radius of 55 nm at 3.5 μg/ml and 34 and 310 nm at 6.0 μg/ml.

Comparison of toxicological responses after exposure in the three exposure systems

First, the toxicity of ZnO NPs was determined across a range of doses to confirm that ZnO NPs could
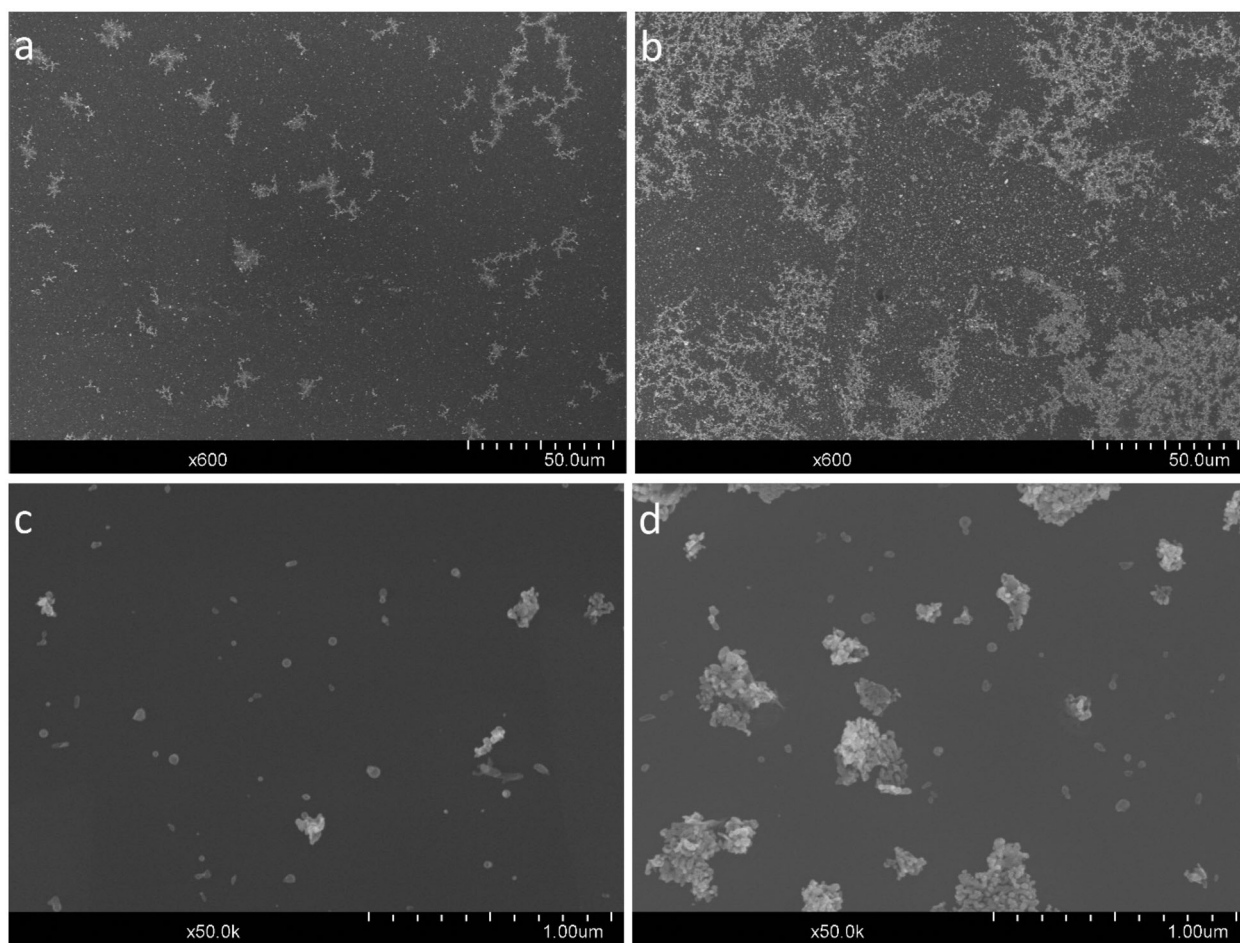
Figure 2. SEM-images of aerosolized ZnO NP deposited on Si wafers in the NACIVT system. (a) Medium dose (x600 magnification), (b) high dose (x600 magnification), (c) medium dose (x50,000 magnification), and (d) high dose (x50,000 magnification).

induce toxicity in the available A549 cells. Metabolic activity was measured in the two submerged systems and across a total of ten doses which covered a range of four orders of magnitude (Figure S3). Dramatic losses of metabolic activity was observed above applied doses of $10 \, \mu g/cm^2$ ZnO NPs, while slight increases in metabolic activity were observed at applied doses below $10 \, \mu g/cm^2$ as compared to unexposed controls (Figure S3). Furthermore, changes in cellular morphology following deposition of ZnO NPs was compared via SEM and cellular blebbing was observed in all exposure conditions, indicative of cell stress (Calcabrini et al. 2004) (Figure S4). This confirms that ZnO NPs can induce cell stress, even at lower concentrations and in the absence of decreased metabolic activity or obvious cell death.

Next, three concentrations were chosen, which are in the range of occupational exposure levels and that could be generated and deposited by the NACIVT system (Table 2). Differences in metabolic activity and cytokine release 24 h after exposure of ZnO NPs were compared between the exposure systems: NACIVT, SUB(iso) and SUB(growth). The medium dose showed a significant increase in metabolic activity, compared to unexposed control, and had higher release of the cytokines IL-8 and MCP-1 in the NACIVT system, while the two submerged systems did not show this effect (Figure 3(a–c)). A significant decrease from unexposed controls could also be seen in the IL-8 levels for the high dose in the SUB(growth) exposure system. Release of IL-8 and MCP-1 was also significantly different between the exposure systems SUB(growth) and NACIVT (Figure 3(b,c)). Additionally, a significant difference between SUB(iso) and NACIVT was seen for MCP-1 release. IL-6 and TNF-α were below the limit of detection in all systems and doses. The LDH assay did not show any cytotoxicity at the studied doses (data not shown).
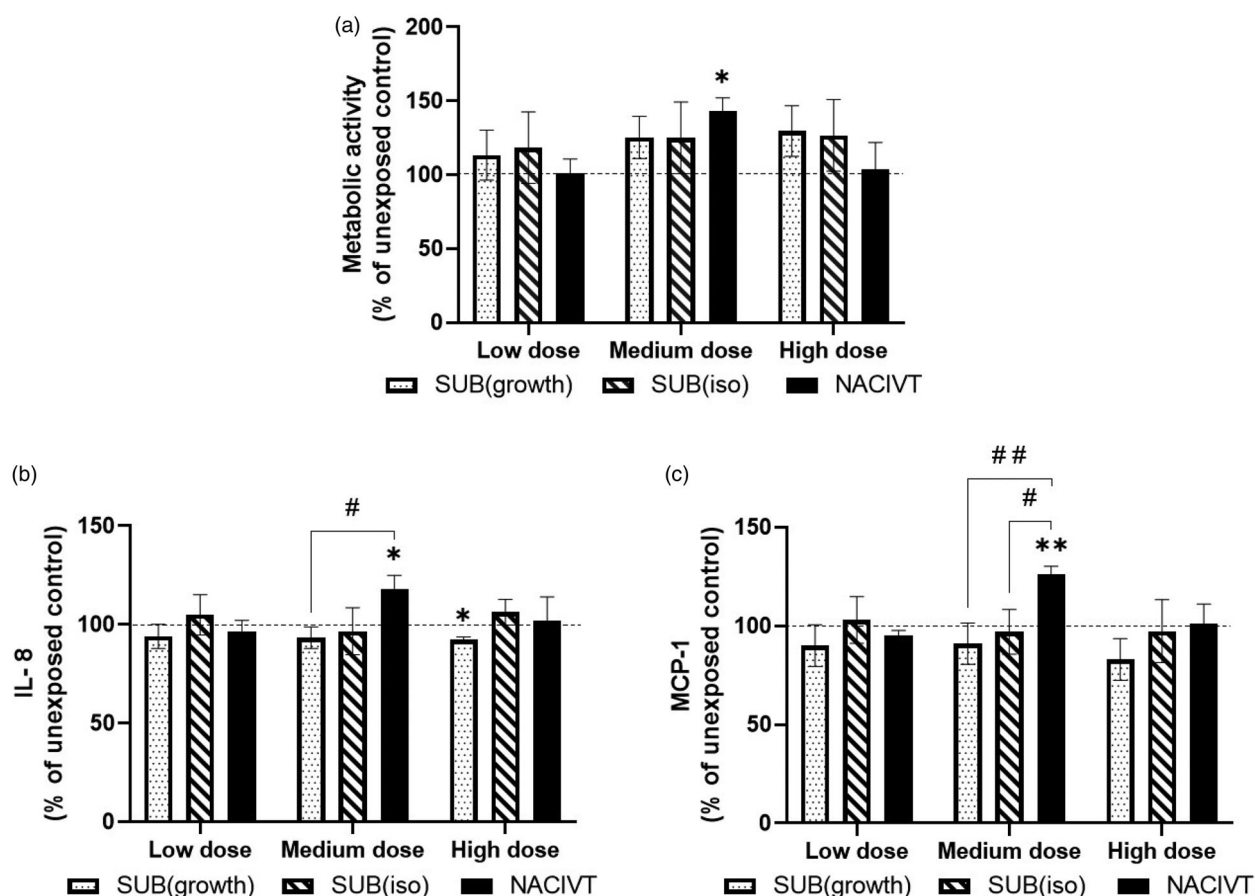
Figure 3. Comparison of toxicological responses after ZnO NP exposures in the three different exposure systems NACIVT, SUB(iso) and SUB(growth) 24 h after exposure. a) Metabolic activity measured with the WST-1 assay, b) IL-8 release measured in basal medium with Multiplexed Luminex, and c) MCP-1 release measured in basal medium with Multiplexed Luminex. The WST-1, IL-8 and MCP-1 results were normalized to the unexposed controls. The symbol (*) indicates significant difference from unexposed control levels at $p < 0.05$ and (**) at $p < 0.01$. The symbol (#) indicates significant difference between exposure systems at $p < 0.05$ and (# #) at $p < 0.01$. The doses corresponded to 0.5, 0.6 and 0.2 $\mu g/cm^2$ (low), 0.9, 1.1 and 1.0 $\mu g/cm^2$ (medium), and 4.5, 4.2 and 3.0 $\mu g/cm^2$ (high) for SUB(growth), SUB(iso) and NACIVT respectively.

Toxicological responses after exposure in the NACIVT system

The toxicological responses were also evaluated at three different time points after ZnO NP exposures in the NACIVT system. Exposure to ZnO NPs at the medium dose showed a significant increase in metabolic activity from unexposed control 3 h after exposure. Additionally, the medium dose showed a significant increase in metabolic activity, and release of the cytokines IL-8 and MCP-1 24 h after exposure (Figure 4(a–c)), compared to unexposed controls. Metabolic activity and the release of MCP-1 were significantly different between the different doses 24 h after exposure (Figure 4(a,c)). A trend of decreasing metabolic activity can be seen with increasing time after exposure to the high doses of ZnO NPs. Similarly to what we observed at the 24 h

time point, IL-6 and TNF-α were below the limit of detection for all doses and time points, and the LDH assay did not show any cytotoxicity at the studied doses (data not shown).

Discussion

This study aimed to evaluate and compare the toxicological responses to ZnO NP exposure in the NACIVT system with two different submerged exposure systems, SUB(iso) and SUB(growth), for three different doses. Due to differences in the anatomy between the lungs of animals and humans, the applicability of aerosol toxicity studies across species is unclear and therefore there is extreme interest in the development and validation of new models which might better represent
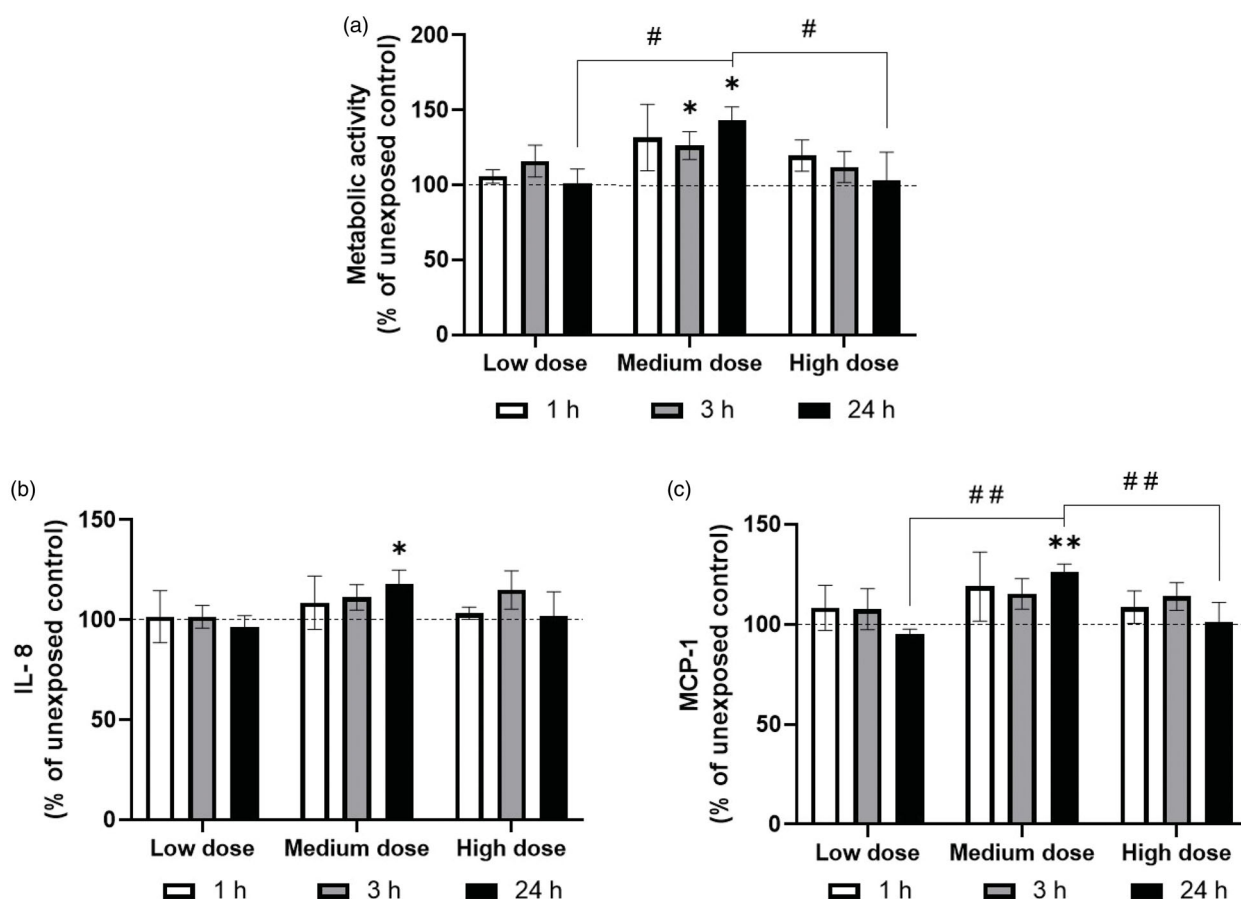
Figure 4. Toxicological responses measured after ZnO NP exposures in the NACIVT system at three different time points after exposure. a) Metabolic activity measured with the WST-1 assay, b) IL-8 release measured in basal medium with Multiplexed Luminex, and c) MCP-1 release measured in basal medium with Multiplexed Luminex. The WST-1, IL-8 and MCP-1 results were normalized to the unexposed controls. The symbol (*) indicates significant difference from unexposed control levels at $p < 0.05$ and (**) at $p < 0.01$. The symbol (#) indicates significant difference between different doses at 24 h after exposure at $p < 0.05$ and (# #) at $p < 0.01$. The doses corresponded to 0.2 (low), 1.0 (medium), and 3.0 μg/cm^2 (high).

human physiological responses. The NACIVT system allows introduction of particles to cells cultured at ALI via aerosolization which more closely resembles the dry exposure of particles often encountered in occupational exposure and pollution settings. Many previous studies have used nebulization based systems which introduces particles in liquid droplets which may also alter particle aggregation and deposition. However, for each of these potential models systems, combinations of particles and cell types need to be validated and compared to traditional submerged culture systems.

In the current study, we showed that the medium dose used in the NACIVT system resulted in a significant increase in the metabolic activity and in the release of the cytokines IL-8 and MCP-1, compared to the unexposed controls. With the same particle size distribution of the aerosol but

with different particle number concentrations, a dose-response relationship for the low and medium dose was found. However, no increase in metabolic activity and cytokine release was further seen for the high dose. Comparing the three exposure systems, a significant difference between the NACIVT and the SUB(growth) exposure system was found for release of the cytokines IL-8 and MCP-1, indicating that the ALI exposure system NACIVT induces different cytokine release levels as compared to the submerged.

In addition to changes in cytokine release, we also observed a significant increase of metabolic activity, compared to unexposed controls, seen for the medium dose ZnO NP exposure in the NACIVT system (Figure 3(a)). However, we did not see further increases at higher doses and did not observe increases in cell death at any of the concentrations

tested, as assessed by the LDH assay. Therefore, this may indicate an initial survival response to subtoxic doses of NPs and a subsequent increase in metabolic activity (Fulda et al. 2010). Increases in metabolic activity at subtoxic levels could be attributed to attempts by the cells to clear NPs which have been internalized, but further studies are needed to better characterize this phenomenon in this exposure system and with these NPs. The high dose exposure in the NACIVT system trended toward a time dependent decrease in metabolic activity (Figure 4(a)) which could suggest that impairment of cellular viability may occur at later time points after ZnO NP exposure. Future studies should include longer timepoints to further assess this.

Increased release of the cytokines IL-8 and MCP-1 after NP exposure is an indication of a toxic response. IL-8 recruits inflammatory cells such as neutrophils (Baggiolini, Walz, and Kunkel 1989), while MCP-1 recruits monocytes/macrophages as a response to inflammation (Deshmane et al. 2009). Only the medium dose exposure of ZnO NPs in the NACIVT system generated an increase of IL-8 and MCP-1 release significantly different to unexposed controls (Figure 3(b,c)). Comparing the exposure systems revealed a significant difference between NACIVT and SUB(growth) for both release of IL-8 and MCP-1, and additionally between NACIVT and SUB(iso) for release of MCP-1.

Several previous studies have compared exposure of ALI cultures to submerged cultures, though not in the NACIVT system. However, the significant increase in release of IL-8, seen for the medium dose (1.0 µg/cm^2) exposure in the NACIVT system in this study, is comparable to previous results presented by Stoehr et al. (2015). They also showed a significant increase in IL-8 release from A549 ALI cultures (ALICE system) after exposure to ZnO NPs, but not in the submerged cultures, though their deposited dose was higher (6.2 µg/cm^2). The increases in IL-8 release was around 2.5-fold (from control cells) 3 h after exposure (non-significant) and about 7-fold 16 h after exposure. The same trend was seen in the current study for the medium dose, where a slight (non-significant) increase could be observed 3 h after exposure and a stronger (about 20%) significant increase was seen 24 h after exposure. The high dose used in the current study (3.0 µg/cm^2) did however not show this increase,

which could be due to a high presence of large aggregates, as we observed in both the SMPS measurements and SEM image analysis of the aerosolized particles. In the report by Stoehr et al., mRNA expression of *IL-8* was also investigated and an increase (non-significant) could be observed for both ALI and submerged cultures 3 h after exposure to the high dose (6.2 µg/cm^2), though with slightly higher levels in ALI cultures. The ALI cultures were also the only ones where increased levels could be found 16 h after exposure (non-significant). Lenz et al. (2013) investigated the mRNA expression of the proinflammatory markers *IL-8*, *IL-6* and *GM-CSF* in A549 cells after ZnO NP exposure and found higher levels in the ALI cultures (MINUCELL system) compared to the submerged for both doses (0.7 and 2.2 µg/cm^2) and both time points tested (0 h and 2 h after exposure). Slight increases in mRNA expression of the oxidative stress markers *GCS*, *SOD-2* and *HMOX-1* could also be observed in the ALI cultures after exposure to ZnO NPs, while only *HMOX-1* increased upon ZnO NPs exposure at the highest dose 2 h after exposure in submerged cultures. In the study by Lenz et al. (2013), multiple proinflammatory and oxidative stress related genes were elevated upon ZnO NP exposure at ALI and *HMOX-1* was the only gene that increased its expression in the submerged condition 2 h after exposure to ZnO NPs. Similarly, in Stoehr et al., only one submerged exposure condition resulted in a more pronounced result in submerged versus ALI (i.e. LDH release 16 h after the high dose exposure (6.2 µg/cm^2)). The increased LDH levels were however, only slightly higher, with about a 3-fold increase in submerged cultures compared to about a 2-fold increase in ALI cultures. The current study, together with the Stoehr et al. (2015) and Lenz et al. (2013) studies, all indicate that ALI culture models are more sensitive to ZnO NP exposure compared to submerged cultures, regardless of which type of ALI exposure system that is used.

A few other studies have compared effects of ZnO NP exposure in ALI and submerged cultures. However, in these studies no clear trend of a stronger ALI sensitivity was observed, but rather different effects were seen after exposure under ALI and submerged conditions respectively (Lenz et al. 2009; Xie et al. 2012; Mihai et al. 2015). In one study, mRNA expression of *IL-8* were similar in A549 cells

under ALI (ALICE system) and submerged conditions, except for the highest dose (5.0 μg/cm^2) where higher levels were observed under submerged conditions. In contrast, higher levels of mRNA expression for the oxidative stress marker *HO-1* were found under ALI conditions (Lenz et al. 2009). In two other studies, mouse alveolar epithelial cells (C10) were used for comparative ALI (Vitrocell systems) and submerged exposures. Xie et al. (2012) showed that the doses needed to achieve a significant deterioration in membrane integrity and cell viability were in the same order of magnitude for both types of exposures. The effects were, though, slightly stronger in the submerged cultures. Mihai et al. (2015) observed similar LDH release levels for both exposure conditions. However, an important finding in this study was the difference in the intracellular Zn^{2+} dynamics between the different exposure conditions, potentially causing differences in the toxic response to ZnO NP exposure. As suggested by these studies, different exposure conditions (ALI versus submerged) could result in differences in the toxicity assessment, which is important to consider when designing and comparing studies and assessing NP toxicity.

Several other more recent studies have also investigated differences between ALI and submerged cultures after exposure to other types of NPs. More pronounced effects were observed in submerged cultures compared to ALI cultures (Vitrocell systems) in two studies after exposure to SiO$_2$ NPs (Panas et al. 2014; Mills-Goodlet et al. 2020). Higher IL-8 and LDH release from A549 cells were seen in Panas et al., although much higher mass dose was used in ALI than in submerged (52 and 15.6 μg/cm^2, respectively). Increased expression of multiple cytokines, for example *IL-8*, in hAELVi (human alveolar epithelial lentivirus immortalized) cells was seen in Mills-Goodlet et al., but where similar dose levels as in the current study were used. However, two other studies showed similar cellular responses in both ALI and submerged cultures, except for in the release of LDH, where higher levels were found in the ALI cultures (Cappellini et al. 2020; Medina-Reyes et al. 2020). These similarities were seen even though several study parameters varied between the two studies. Cappellini et al. exposed co-cultures of A549 and

THP-1 (macrophages) cells to CeO$_2$ NPs and observed higher LDH levels at a dose of 5 μg/cm^2 in the ALI cultures (XposeALI system), while Medina-Reyes et al. exposed A549 cells to TiO$_2$ NPs and nanofibers (NFs) and observed higher LDH levels at a dose of 10 μg/cm^2 in the ALI cultures (Vitrocell system). Additional studies have observed different results in ALI cultures (Vitrocell systems) compared to submerged, with exceeding responses in ALI cultures. Increased cytokine levels (of for example IL-8) were seen at lower doses in ALI than in submerged (1 and 3 μg/cm^2, respectively) after TiO$_2$ and CeO$_2$ NP exposure to co-cultures of A549 and THP-1 cells (Loret et al. 2016). Expression of several proteins (for example *SOD-2*, associated with an oxidative stress response) were found to be significantly increased in ALI cultures, but not in submerged after MWCNT (multi walled carbon nanotube) exposure to co-cultures of A549, THP-1 and MRC-5 (fibroblasts) (Hilton et al. 2019). These increases were detected even though a lower dose was used in ALI compared to in submerged (10 and 18 μg/cm^2, respectively). Taking all these comparative studies together, it could be argued that the use of ALI exposure systems provide a more sensitive assay for toxicity assessment of ENM exposure, and since they seem to respond to lower doses, they could be more realistic for occupational exposure.

A few other studies have also indicated larger effects in ALI compared to submerged cultures after exposure to different chemicals (not NPs), such as sodium metavanadate and carbendazim (Gohlsch et al. 2019; Tollstadius et al. 2019; Hu et al. 2020). Additionally, Ohlinger et al. (2019) have shown that culturing A549 cells at ALI increased the expression of several alveolar type II specific genes (for example *SLCO2B1*, *ALB*, *CYP3A5*, *CFI*) compared to when cultured in submerged, further indicating the advantages with ALI culture exposures, which more readily allows the effects of NPs on alveolar type II cell behavior. Future developments of ENM respiratory exposure models could also combine ALI cultures with mechanical stretch (simulating breathing) for even more realistic evaluations (Doryab et al. 2019). Another approach could be to use primary lung epithelial cells and other lung resident cell types (for example fibroblasts, macrophages etc.) or those derived from induced pluripotent stem cells.

Primary cells are known to be more sensitive to external stimuli than cell lines, such as A549, and may therefore be a preferred cell type if they can be sourced.

Some limitations of the current study design exist for the submerged as well as for the NACIVT system experiments. In the two submerged systems, different suspension liquids were used in SUB(iso) and SUB(growth): 0.9% NaCl isotonic solution and serum-containing growth medium, respectively. According to Peng et al. (2017), micro-sized ZnO aggregates form at NaCl concentrations higher than 6 meq/l. In the current study, a 0.9% NaCl isotonic solution was used (corresponding to 154 meq/l), indicating that there was potential formation of micro-sized aggregates in the isotonic suspension. DLS analysis indicated the presence of large aggregates in both the isotonic and the serum-containing growth medium suspensions. Additionally, to achieve the same deposited dose, different concentrations had to be used in the two submerged systems, potentially leading to higher aggregate sizes in the isotonic solutions as compared to aggregates in the growth medium at similar applied doses. A lower volume of ZnO NP suspension in the SUB(iso) system was chosen to resemble cells at the ALI as closely as possible. The difference in particle concentrations as well as the differing degree of aggregation due to the different suspension liquids could have resulted in different aggregate sizes which can affect several parameters such as the deposited mass dose and the type of cellular uptake (i.e. endocytosis, phagocytosis, macropinocytosis and pinocytosis). Together, the deposited dose and particle uptake mechanism have a major impact on the final toxicological effect in these two exposure systems. Another factor influencing the final deposited mass dose in these two systems was the ratio of available cell to wall area, calculated by estimating the height of the liquid pillar on the apical side of the cells. In the SUB(iso) system, this ratio was 2.67 while in the SUB(growth) system only 1.07. This could have affected the possibility for particle losses due to diffusion and adhesion to the insert walls (Upadhyay and Palmberg 2018), possibly leading to an overestimation of the final deposited mass dose. However, as described previously, the gravitational settling of the ZnO NPs is expected to be more dominant than diffusional displacement

(Stoehr et al. 2015) and ZnO NPs have been previously shown to be deposited with nearly 100% efficiency after 1 h through a 50 mm liquid depth (Lenz et al. 2013). The current study anticipated the same behavior based on large aggregation sizes determined by DLS measurements (which was also indicated in the SEM images, Figure S4), a lower depth of the suspensions (0.6 mm and 1.5 mm for SUB(iso) and SUB(growth) respectively) and a longer exposure time (24 h). Even if the sedimentation rate in reality would be lower than what we assumed here – if for example considering the fact that the shape of the aggregates would result in a lower effective density than the bulk material, as exemplified by Deloid et al. (2014) – it is still reasonable to assume a particle deposition of 100% in the current study. This since the total gravitational settling time would be well in the time frame of the 24 h exposure.

In the NACIVT exposures, different aerosol aggregate sizes were seen both with the SMPS (Figure 1) and in the SEM (Figure 2) for the high dose compared to the low and medium dose. For the high dose, the aggregate sizes were larger than for the low and medium doses and fewer single particles were present. The small size of the individual ZnO NPs or the dissolution of aggregates into single ZnO NPs for cellular uptake could have influenced the cellular responses, since smaller particles have been shown to induce greater toxicological responses (Wang et al. 2018).

To calculate the surface area doses, the SSA was determined from an estimated primary particle size, which introduces an uncertainty in the used SSA. Another uncertainty introduced in these calculations is applying the SSA determined for the primary particles also to the aggregates formed. If the primary particles are at point contact, this approach will not introduce any errors, however, if the primary particles are partly fused, the SSA is overestimated. Based on the discussion and calculations made by Svensson et al. (2015), the overestimation of the SSA would however be less than 20% (20% corresponds to when the diameter of the bridge is 60-70% of the diameter of the primary particles, for open aggregates). Another error possibly introduced is assuming that the densities of the primary particles are equal to that of the ZnO bulk. Typically, due to the high curvature of the surface of nanoparticles, the density is somewhat lower.

This may lead to an underestimation of the SSA. The argument regarding the density of nanoparticles also applies to the mass dose calculations for the NACIVT system, which can lead to an overestimation of these mass doses.

In this study, metabolic activity, cytotoxicity and release of the cytokines IL-8, MCP-1, IL-6 and TNF-α were evaluated after ZnO NP exposure in the ALI exposure system NACIVT, and compared with two different submerged exposure systems, SUB(iso) and SUB(growth). Our findings suggest that exposure via the NACIVT system induces different cellular responses (metabolic activity and cytokine release) than exposure in the two submerged systems at similar exposure doses, with toxicity reactions at lower doses in the ALI cultures than in submerged. The agreement between our results and several previous studies (Lenz et al. 2013; Stoehr et al. 2015; Loret et al. 2016; Hilton et al. 2019), encourages the future use of more physiologically realistic exposure systems for testing cellular responses to ENMs, as well as continued comparisons with traditionally submerged systems.

Acknowledgments

Disclosure statement

Funding

ORCID

Karin Lovén http://orcid.org/0000-0003-3837-8124
Deniz A. Bölükbas http://orcid.org/0000-0002-5034-4245
Monica Kåredal http://orcid.org/0000-0002-5936-2829
Sinem Tas http://orcid.org/0000-0003-0691-8157
Jenny Rissler http://orcid.org/0000-0001-8650-4741
Darcy E. Wagner http://orcid.org/0000-0003-3794-1309
Christina Isaxon http://orcid.org/0000-0002-9105-4017

References

Ambade, S. B., R. S. Mane, A. V. Ghule, M. G. Takwale, A. Abhyankar, B. Cho, and S. H. Han. 2009. "Contact Angle Measurement: A Preliminary Diagnostic Method for Evaluating the Performance of ZnO Platelet-Based Dye-Sensitized Solar Cells." *Scripta Materialia* 61 (1): 12–15. doi:10.1016/j.scriptamat.2009.02.011.

Aufderheide, M., S. Scheffler, N. Mohle, B. Halter, and D. Hochrainer. 2011. "Analytical In Vitro Approach for Studying Cyto- and Genotoxic Effects of Particulate Airborne Material." *Analytical and Bioanalytical Chemistry* 401 (10): 3213–3220. doi:10.1007/s00216-011-5163-4.

Baggiolini, M., A. Walz, and S. L. Kunkel. 1989. "Neutrophil-Activating Peptide-1 Interleukin-8, a Novel Cytokine That Activates Neutrophils." *Journal of Clinical Investigation* 84 (4): 1045–1049. doi:10.1172/JCI114265.

Basinas, I., A. S. Jimenez, K. S. Galea, M. VAN Tongeren, and F. Hurley. 2018. "A Systematic Review of the Routes and Forms of Exposure to Engineered Nanomaterials." *Annals of Work Exposures and Health* 62 (6): 639–662. doi:10.1093/annweh/wxy048.

Calcabrini, A., S. Meschini, M. Marra, L. Falzano, M. Colone, B. DE Berardis, L. Paoletti, G. Arancia, and C. Fiorentini. 2004. "Fine Environmental Particulate Engenders Alterations in Human Lung Epithelial A549 Cells." *Environmental Research* 95 (1): 82–91.

Cappellini, F., S. DI Bucchianico, V. Karri, S. Latvala, M. Malmlof, M. Kippler, K. Elihn, et al. 2020. "Dry Generation of CeO2 Nanoparticles and Deposition onto a Co-Culture of A549 and THP-1 Cells in Air-Liquid Interface-Dosimetry Considerations and Comparison to Submerged Exposure." *Nanomaterials* 10 (4): 618. doi:10.3390/nano10040618.

Chen, J. K., C. C. Ho, H. Chang, J. F. Lin, C. S. Yang, M. H. Tsai, H. T. Tsai, and P. P. Lin. 2015. "Particulate Nature of Inhaled Zinc Oxide Nanoparticles Determines Systemic Effects and Mechanisms of Pulmonary Inflammation in Mice." *Nanotoxicology* 9 (1): 43–53. doi:10.3109/17435390.2014.886740.

Cho, W. S., R. Duffin, S. E. M. Howie, C. J. Scotton, W. A. H. Wallace, W. Macnee, M. Bradley, I. L. Megson, and K. Donaldson. 2011. "Progressive Severe Lung Injury by Zinc Oxide Nanoparticles; the Role of Zn2+ Dissolution inside Lysosomes." *Particle and Fibre Toxicology* 8: 27.

Delaval, M., D. Egli, P. Schupfer, C. Benarafa, M. Geiser, and H. Burtscher. 2019. "Novel Instrument to Generate Representative e-Cigarette Vapors for Physicochemical

Particle Characterization and In-Vitro Toxicity." *Journal of Aerosol Science* 129: 40–52. doi:10.1016/j.jaerosci.2018.11.011.

Deloid, G., J. M. Cohen, T. Darrah, R. Derk, L. Rojanasakul, G. Pyrgiotakis, W. Wohlleben, and P. Demokritou. 2014. "Estimating the Effective Density of Engineered Nanomaterials for In Vitro Dosimetry." *Nature Communications* 5 (1): 3514. doi:10.1038/ncomms4514.

Deshmane, S. L., S. Kremlev, S. Amini, and B. E. Sawaya. 2009. "Monocyte Chemoattractant Protein-1 (MCP-1): An Overview." *Journal of Interferon & Cytokine Research* 29 (6): 313–326. doi:10.1089/jir.2008.0027.

Doryab, A., S. Tas, M. B. Taskin, L. Yang, A. Hilgendorff, J. Groll, D. E. Wagner, and O. Schmid. 2019. "Evolution of Bioengineered Lung Models: Recent Advances and Challenges in Tissue Mimicry for Studying the Role of Mechanical Forces in Cell Biology." *Advanced Functional Materials* 29 (39): 1903114. doi:10.1002/adfm.201903114.

Fulda, S., A. M. Gorman, O. Hori, and A. Samali. 2010. "Cellular Stress Responses: Cell Survival and Cell Death." *International Journal of Cell Biology* 2010: 1–23. 2010. doi:10.1155/2010/214074.

Geiser, M., N. Jeannet, M. Fierz, and H. Burtscher. 2017. "Evaluating Adverse Effects of Inhaled Nanoparticles by Realistic In Vitro Technology." *Nanomaterials* 7 (2): 49.

Gohlsch, K., H. Muckter, D. Steinritz, M. Aufderheide, S. Hoffmann, T. Gudermann, and A. Breit. 2019. "Exposure of 19 Substances to Lung A549 Cells at the Air Liquid Interface or under Submerged Conditions Reveals High Correlation between Cytotoxicity In Vitro and CLP Classifications for Acute Lung Toxicity." *Toxicology Letters* 316: 119–126. doi:10.1016/j.toxlet.2019.09.014.

Hilton, G., H. Barosova, A. Petri-Fink, B. Rothen-Rutishauser, and M. Bereman. 2019. "Leveraging Proteomics to Compare Submerged versus Air-Liquid Interface Carbon Nanotube Exposure to a 3D Lung Cell Model." *Toxicology In Vitro* 54: 58–66. doi:10.1016/j.tiv.2018.09.010.

Hu, Y., Y. H. Sheng, X. L. Ji, P. Liu, L. M. Tang, G. Chen, and G. L. Chen. 2020. "Comparative anti-Inflammatory Effect of Curcumin at Air-Liquid Interface and Submerged Conditions Using Lipopolysaccharide Stimulated Human Lung Epithelial A549 Cells." *Pulmonary Pharmacology & Therapeutics* 63: 101939. doi:10.1016/j.pupt.2020.101939.

Jeannet, N., M. Fierz, M. Kalberer, H. Burtscher, and M. Geiser. 2015. "Nano Aerosol Chamber for In-Vitro Toxicity (NACIVT) Studies." *Nanotoxicology* 9 (1): 34–42. doi:10.3109/17435390.2014.886739.

Jeannet, N., M. Fierz, S. Schneider, L. Kunzi, N. Baumlin, M. Salathe, H. Burtscher, and M. Geiser. 2016. "Acute Toxicity of Silver and Carbon Nanoaerosols to Normal and Cystic Fibrosis Human Bronchial Epithelial Cells." *Nanotoxicology* 10 (3): 279–291. doi:10.3109/17435390.2015.1049233.

Ji, J., A. Hedelin, M. Malmlof, V. Kessler, G. Seisenbaeva, P. Gerde, and L. Palmberg. 2017. "Development of Combining of Human Bronchial Mucosa Models with XposeALI (R) for Exposure of Air Pollution Nanoparticles." *PLos One* 12 (1): e0170428.

Jiang, C. J., G. R. Aiken, and H. Hsu-Kim. 2015. "Effects of Natural Organic Matter Properties on the Dissolution Kinetics of Zinc Oxide Nanoparticles." *Environmental Science & Technology* 49 (19): 11476–11484. doi:10.1021/acs.est.5b02406.

Kumar, S. A., and S. M. Chen. 2008. "Nanostructured Zinc Oxide Particles in Chemically Modified Electrodes for Biosensor Applications." *Analytical Letters* 41 (2): 141–158. doi:10.1080/00032710701792612.

Larsen, S. T., E. Da Silva, J. S. Hansen, A. C. O. Jensen, I. K. Koponen, and J. B. Sorli. 2020. "Acute Inhalation Toxicity after Inhalation of ZnO Nanoparticles: Lung Surfactant Function Inhibition In Vitro Correlates with Reduced Tidal Volume in Mice." *International Journal of Toxicology* 39 (4): 321–327. doi:10.1177/1091581820933146.

Lenz, A. G., E. Karg, E. Brendel, H. Hinze-Heyn, K. L. Maier, O. Eickelberg, T. Stoeger, and O. Schmid. 2013. "Inflammatory and Oxidative Stress Responses of an Alveolar Epithelial Cell Line to Airborne Zinc Oxide Nanoparticles at the Air-Liquid Interface: A Comparison with Conventional, Submerged Cell-Culture Conditions." *BioMed Research International* 2013: 652632. doi:10.1155/2013/652632.

Lenz, A. G., E. Karg, B. Lentner, V. Dittrich, C. Brandenberger, B. Rothen-Rutishauser, H. Schulz, G. A. Ferron, and O. Schmid. 2009. "A Dose-Controlled System for Air-Liquid Interface Cell Exposure and Application to Zinc Oxide Nanoparticles." *Particle and Fibre Toxicology* 6 (1): 32. doi:10.1186/1743-8977-6-32.

Lewicka, Z. A., A. F. Benedetto, D. N. Benoit, W. W. Yu, J. D. Fortner, and V. L. Colvin. 2011. "The Structure, Composition, and Dimensions of TiO2 and ZnO Nanomaterials in Commercial Sunscreens." *Journal of Nanoparticle Research* 13 (9): 3607–3617. doi:10.1007/s11051-011-0438-4.

Loret, T., E. Peyret, M. Dubreuil, O. Aguerre-Chariol, C. Bressot, O. Le Bihan, T. Amodeo, et al. 2016. "Air-Liquid Interface Exposure to Aerosols of Poorly Soluble Nanomaterials Induces Different Biological Activation Levels Compared to Exposure to Suspensions." *Particle and Fibre Toxicology* 13 (1): 58. doi:10.1186/s12989-016-0171-3.

Lucci, F., N. D. Castro, A. A. Rostami, M. J. Oldham, J. Hoeng, Y. B. Pithawalla, and A. K. Kuczaj. 2018. "Characterization and Modeling of Aerosol Deposition in Vitrocell (R) exposure Systems - Exposure Well Chamber Deposition Efficiency." *Journal of Aerosol Science* 123: 141–160. doi:10.1016/j.jaerosci.2018.06.015.

Medina-Reyes, E. I., N. L. Delgado-Buenrostro, D. L. Leseman, A. Déciga-Alcaraz, R. He, E. R. Gremmer, P. H. B. Fokkens, J. O. Flores-Flores, F. R. Cassee, and Y. I. Chirino. 2020. "Differences in Cytotoxicity of Lung Epithelial Cells Exposed to Titanium Dioxide Nanofibers and Nanoparticles: Comparison of Air-Liquid Interface and Submerged Cell Cultures." *Toxicology In Vitro* 65: 104798. doi:10.1016/j.tiv.2020.104798.

Mihai, C., W. B. Chrisler, Y. M. Xie, D. H. Hu, C. J. Szymanski, A. Tolic, J. A. Klein, J. N. Smith, B. J. Tarasevich, and G. Orr. 2015. "Intracellular Accumulation Dynamics and Fate of Zinc Ions in Alveolar Epithelial Cells Exposed to Airborne ZnO Nanoparticles at the Air-Liquid Interface." *Nanotoxicology* 9 (1): 9–22. doi:10.3109/17435390.2013.859319.

Mills-Goodlet, R., M. Schenck, A. Chary, M. Geppert, T. Serchi, S. Hofer, N. Hofstatter, et al. 2020. "Biological Effects of Allergen-Nanoparticle Conjugates: Uptake and Immune Effects Determined on hAELVi Cells under Submergedvs.air-Liquid Interface Conditions." *Environmental Science: Nano* 7 (7): 2073–2086. doi:10.1039/C9EN01353A.

Ohlinger, K., T. Kolesnik, C. Meindl, B. Galle, M. Absenger-Novak, D. Kolb-Lenz, and E. Frohlich. 2019. "Air-Liquid Interface Culture Changes Surface Properties of A549 Cells." *Toxicology In Vitro* 60: 369–382. doi:10.1016/j.tiv.2019.06.014.

Panas, A., A. Comouth, H. Saathoff, T. Leisner, M. Al-Rawi, M. Simon, G. Seemann, et al. 2014. "Silica Nanoparticles Are Less Toxic to Human Lung Cells When Deposited at the Air-Liquid Interface Compared to Conventional Submerged Exposure." *Beilstein Journal of Nanotechnology* 5: 1590–1602. doi:10.3762/bjnano.5.171.

Peng, Y. H., Y. C. Tsai, C. E. Hsiung, Y. H. Lin, and Y. H. Shih. 2017. "Influence of Water Chemistry on the Environmental Behaviors of Commercial ZnO Nanoparticles in Various Water and Wastewater Samples." *Journal of Hazardous Materials* 322 (Pt B): 348–356. doi:10.1016/j.jhazmat.2016.10.003.

Piccinno, F., F. Gottschalk, S. Seeger, and B. Nowack. 2012. "Industrial Production Quantities and Uses of Ten Engineered Nanomaterials in Europe and the World." *Journal of Nanoparticle Research* 14: 1109.

Raemy, D. O., R. N. Grass, W. J. Stark, C. M. Schumacher, M. J. D. Clift, P. Gehr, and B. Rothen-Rutishauser. 2012. "Effects of Flame Made Zinc Oxide Particles in Human Lung Cells - a Comparison of Aerosol and Suspension Exposures." *Particle and Fibre Toxicology* 9 (1): 33. doi:10.1186/1743-8977-9-33.

Secondo, L. E., N. J. Liu, and N. A. Lewinski. 2017. "Methodological Considerations When Conducting In Vitro, Air-Liquid Interface Exposures to Engineered Nanoparticle Aerosols." *Critical Reviews in Toxicology* 47 (3): 225–262. doi:10.1080/10408444.2016.1223015.

Sharma, D., J. Rajput, B. S. Kaith, M. Kaur, and S. Sharma. 2010. "Synthesis of ZnO Nanoparticles and Study of Their Antibacterial and Antifungal Properties." *Thin Solid Films.* 519 (3): 1224–1229. doi:10.1016/j.tsf.2010.08.073.

Srivastava, V., D. Gusain, and Y. C. Sharma. 2015. "Critical Review on the Toxicity of Some Widely Used Engineered Nanoparticles." *Industrial & Engineering Chemistry Research* 54 (24): 6209–6233. doi:10.1021/acs.iecr.5b01610.

Stoehr, L. C., C. Endes, I. Radauer-Preiml, M. S. P. Boyles, E. Casals, S. Balog, M. Pesch, et al. 2015. "Assessment of a Panel of Interleukin-8 Reporter Lung Epithelial Cell Lines to Monitor the Pro-Inflammatory Response following Zinc Oxide Nanoparticle Exposure under Different Cell Culture Conditions." *Particle and Fibre Toxicology* 12: 29. doi:10.1186/s12989-015-0104-6.

Svensson, C. R., S. S. Ameer, L. Ludvigsson, N. Ali, A. Alhamdow, M. E. Messing, J. Pagels, A. Gudmundsson, et al. 2016. "Validation of an Air-Liquid Interface Toxicological Set-up Using Cu, Pd, and Ag Well-Characterized Nanostructured Aggregates and Spheres." *Journal of Nanoparticle Research* 18 (4): 86. doi:10.1007/s11051-016-3389-y.

Svensson, C. R., L. Ludvigsson, B. O. Meuller, M. L. Eggersdorfer, K. Deppert, M. Bohgard, J. H. Pagels, M. E. Messing, and J. Rissler. 2015. "Characteristics of Airborne Gold Aggregates Generated by Spark Discharge and High Temperature Evaporation Furnace: Mass-Mobility Relationship and Surface Area." *Journal of Aerosol Science* 87: 38–52. doi:10.1016/j.jaerosci.2015.05.004.

Thongkam, W., K. Gerloff, D. VAN Berlo, C. Albrecht, and R. P. F. Schins. 2017. "Oxidant Generation, DNA Damage and Cytotoxicity by a Panel of Engineered Nanomaterials in Three Different Human Epithelial Cell Lines." *Mutagenesis* 32 (1): 105–115. doi:10.1093/mutage/gew056.

Tollstadius, B. F., A. C. G. Da Silva, B. C. O. Pedralli, and M. C. Valadares 2019. "Carbendazim Induces Death in Alveolar Epithelial Cells: A Comparison between Submerged and at the Air-Liquid Interface Cell Culture." *Toxicology In Vitro* 58: 78–85. doi:10.1016/j.tiv.2019.03.004.

Upadhyay, S., and L. Palmberg. 2018. "Air-Liquid Interface: Relevant In Vitro Models for Investigating Air Pollutant-Induced Pulmonary Toxicity." *Toxicological Sciences* 164 (1): 21–30. doi:10.1093/toxsci/kfy053.

Vandebriel, R. J., and W. H. De Jong. 2012. "A Review of Mammalian Toxicity of ZnO Nanoparticles." *Nanotechnology, Science and Application* 5: 61–71.

Wang, B., J. Zhang, C. Z. Chen, G. Xu, X. Qin, Y. L. Hong, D. D. Bose, F. Qiu, and Z. Zou. 2018. "The Size of Zinc Oxide Nanoparticles Controls Its Toxicity through Impairing Autophagic Flux in A549 Lung Epithelial Cells." *Toxicology Letters* 285: 51–59. doi:10.1016/j.toxlet.2017.12.025.

Wang, P., N. W. Menzies, E. Lombi, B. A. Mckenna, B. Johannessen, C. J. Glover, P. Kappen, and P. M. Kopittke. 2013. "Fate of ZnO Nanoparticles in Soils and Cowpea (Vigna unguiculata)." *Environmental Science & Technology* 47 (23): 13822–13830. doi:10.1021/es403466p.

Warheit, D. B., C. M. Sayes, and K. L. Reed. 2009. "Nanoscale and Fine Zinc Oxide Particles: Can In Vitro Assays Accurately Forecast Lung Hazards following Inhalation Exposures?" *Environmental Science & Technology* 43 (20): 7939–7945. doi:10.1021/es901453p.

Xie, Y. M., N. G. Williams, A. Tolic, W. B. Chrisler, J. G. Teeguarden, B. L. S. Maddux, J. G. Pounds, A. Laskin, and G. Orr. 2012. "Aerosolized ZnO Nanoparticles Induce Toxicity in Alveolar Type II Epithelial Cells at the Air-Liquid Interface." *Toxicological Sciences* 125 (2): 450–461. doi:10.1093/toxsci/kfr251.